

LEVEL II

12
NW

ARL-MAT-REPORT-103

AR-001-273



**DEPARTMENT OF DEFENCE
DEFENCE SCIENCE AND TECHNOLOGY ORGANISATION
AERONAUTICAL RESEARCH LABORATORIES
MELBOURNE, VICTORIA**

ADA062571

MATERIALS REPORT 103

**MECHANISMS OF HYDROGEN EMBRITTLEMENT—
CRACK GROWTH IN A LOW-ALLOY
ULTRA-HIGH-STRENGTH STEEL UNDER CYCLIC AND
SUSTAINED STRESSES IN GASEOUS HYDROGEN**

DDC FILE COPY

by

S. P. LYNCH and N. E. RYAN

Reproduced From
Best Available Copy

APPROVED FOR PUBLIC RELEASE



DDC
REFRAME
DEC 21 1978
REGISTERED
D

© COMMONWEALTH OF AUSTRALIA 1978

COPY No

7

MAY 1978

72 12 15 027

APPROVED

FOR PUBLIC RELEASE

THE UNITED STATES NATIONAL
TECHNICAL INFORMATION SERVICE
IS AUTHORISED TO
REPRODUCE AND SELL THIS REPORT

Reproduced From
Best Available Copy

APPROVAL BY	
STS	White Section <input checked="" type="checkbox"/>
DPS	Defi Section <input type="checkbox"/>
CHANGED	<input type="checkbox"/>
JUSTIFICATION	
BY	
DISTRIBUTION/AVAILABILITY CODES	
OSL	AVAIL. MOD./W. SPECIAL
A	

LEVEL II

AR-001-273

DEPARTMENT OF DEFENCE
DEFENCE SCIENCE AND TECHNOLOGY ORGANISATION
AERONAUTICAL RESEARCH LABORATORIES

MATERIALS REPORT 103

MECHANISMS OF HYDROGEN EMBRITTLEMENT— CRACK GROWTH IN A LOW-ALLOY ULTRA-HIGH-STRENGTH STEEL UNDER CYCLIC AND SUSTAINED STRESSES IN GASEOUS HYDROGEN

by

10 S. P. LYNCH and N. E. RYAN

1023 p.

SUMMARY

Rates of crack growth in a low-alloy ultra-high-strength steel (D6aC) under cyclic and sustained stresses have been measured as functions of stress-intensity, for different cyclic wave-forms and frequencies, in low pressure (13.3 kPa) hydrogen, dry air, and vacuum (10^{-3} Pa) environments; sustained-load cracking in liquid mercury was also studied.

Frequency and wave-form had large effects on rates of fatigue-crack growth in hydrogen but little influence on fatigue in air and vacuum. For triangular wave-forms, rates of crack growth in hydrogen were determined mainly by the stress-intensity range and the load-rise time. For square-wave loading, rates of crack growth in hydrogen were proportional to the time at maximum load. Quantitative relationships between rates of cracking under sustained and cyclic loads were not found.

Many similarities between hydrogen-embrittlement and liquid-metal embrittlement (e.g. surfaces of the intercrystalline fractures induced by hydrogen and mercury were sometimes indistinguishable), suggested that the mechanism of embrittlement is basically the same in both cases. It is considered that previous explanations for embrittlement are not consistent with the present fractographic observations (e.g. dimpled transcrystalline fractures were sometimes observed after crack growth in mercury and hydrogen). The present results suggest that the effects of hydrogen and liquid-metal environments on crack growth can generally be explained on the basis that chemisorption influences interatomic bonds/spacings at surfaces (crack tips) and thereby facilitates nucleation of dislocations at crack tips. Some aspects of hydrogen embrittlement are discussed in terms of the proposed model.

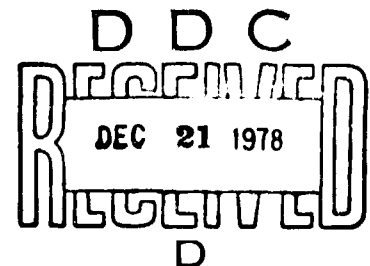
Reproduced From
Best Available Copy

POSTAL ADDRESS: Chief Superintendent, Aeronautical Research Laboratories,
Box 4331, P.O., Melbourne, Victoria, 3001, Australia.

78 12 15 027

CONTENTS

1. INTRODUCTION	1
2. EXPERIMENTAL	1-2
3. RESULTS	2
3.1 Crack-Growth Data	2
3.2 Fractography	2
3.2.1 Sustained-Load Cracking in Hydrogen	2
3.2.2 Sustained-Load Cracking in Liquid Mercury	2-3
3.2.3. Fatigue in Dry Air	3
3.2.4 Fatigue in Hydrogen	3
4. DISCUSSION	3
4.1 Previous Explanations for Hydrogen Embrittlement (HE)	3-4
4.2 Comparison of HE and LME	4
4.3 A New Explanation for HE and LME	4-5
4.4 Explanation of Some Aspects of HE	5
4.4.1 Environmental Factors—Effect of Oxygen, Solute Elements on HE	5-6
4.4.2 Ductile versus Brittle Behaviour	6
4.4.3 Effect of Hydrogen on Rates of Crack Growth	6-7
4.4.4 Relation between Sustained-and Cyclic-Load Cracking	7
5. CONCLUSIONS	7
REFERENCES	
FIGURES	
DISTRIBUTION	



1. INTRODUCTION

In high-strength steels, hydrogen environments induce sub-critical crack growth under sustained stress and can increase the rates of crack growth under cyclic stress markedly beyond those in inert environments. Some aspects of these and other effects of hydrogen on the behaviour of materials are discussed in references 1 and 2. The present studies of crack growth as a function of stress intensity under (a) cyclic stress in 'inert' environments (fatigue), (b) cyclic stress in hydrogen ('corrosion-fatigue'), (c) sustained stress in hydrogen, and (d) sustained stress in liquid mercury were undertaken to investigate possible relationships between these cracking processes. If relationships between (a), (b), and (c) above could be established, they would provide a basis for using existing data on fatigue and sustained-load cracking to predict rates of 'corrosion-fatigue' without the necessity for empirical testing. It was also considered that the results would be relevant to understanding mechanisms of hydrogen-assisted crack growth.

2. EXPERIMENTAL

Specimens were manufactured from 22 mm thick D6aC steel plate of the following composition:

C	Mo	Cr	Ni	V	Mn	Si	P	S	Fe
0.46	1.2	1.1	0.6	0.12	0.8	0.24	0.004	0.002	rem. wt. %

They were austenitised at 930°C, quenched in molten salt at 520°C ('Ausbay' region), held at 520°C for 25 min., quenched in molten salt at 210°C, and then double-tempered at 550°C for 2 hr. This heat-treatment produces a tempered-martensitic (predominantly lath-type) microstructure. Mechanical properties were as follows:

0.2% Proof Stress (MPa)	UTS (MPa)	Elongation (%)	Reduction of Area (%)	K_{Ic} (MPa m ^{1/2})
1460	1650	12	43	78

A few sustained-load tests in liquid mercury were also carried out on specimens additionally tempered at either 625°C for 4 hr. or 650°C for 4 hr giving proof stresses of ~1250 MPa and ~1000 MPa, respectively.

Crack growth in the gaseous environments was studied using tapered double-cantilever-beam (DCB) specimens. For this specimen geometry, the crack-tip stress intensity is independent of crack length over a considerable portion of the specimen. Specimens were enclosed in an environmental chamber which could be evacuated to 10⁻³ Pa and then filled with gases. High purity hydrogen with O₂, N₂, and H₂O contents of less than 10, 100, and 200 ppm respectively, and dry air with a water-vapour content of less than 25 ppm were used. Hydrogen gas was chosen as a 'model' aggressive environment which induces less complex conditions at crack tips than aqueous media, where electrochemical reactions could produce a variety of effects. A hydrogen pressure of 13.3 kPa was used, giving rates of fatigue-crack growth (which increase with increasing pressure) in the range 0.1 to 100 μm per cycle; slower and faster rates are wasteful of testing time and specimens, respectively.

Specimens were tested at 25°C using a closed-loop electrohydraulic machine operating under load control. Rates of fatigue-crack growth (da/dN) were measured as a function of stress-intensity range (ΔK), for a stress ratio of ~0.1, in dry air, vacuum (10⁻³ Pa) and hydrogen (13.3 kPa) using four wave-forms and four to five frequencies, from 5 Hz to 0.02 Hz. The wave-forms used were (a) triangular (Δ), (b) 'positive' saw-tooth (\sphericalangle), (c) 'negative' saw-tooth (∇), with loading-to-unloading times in the ratios 1:1, 10:1, and 1:10 respectively, and (d) 'square' (\square) with loading/unloading times ~0.02 sec. Rates of crack growth were determined from direct observation of crack lengths on the sides of specimens and also by compliance

measurements—a calibration curve of crack-opening displacement versus crack length had been established previously.

Sustained-load cracking in liquid mercury (at 25°C) was studied using parallel-sided bolt-loaded DCB specimens at constant crack-opening displacement (COD), for which the crack-tip stress intensity decreases with increasing crack length. Mercury was applied to specimens by drilling a small shallow hole through a pool of mercury just ahead of the chevron notch. On loading, fracture initially occurred in air under continuously increasing COD until the crack tip intersected the area 'wetted' by mercury; rapid sub-critical crack growth, under a constant COD, then occurred. Mercury was removed from the fracture by evaporation in vacuum at ~100°C. Fracture surfaces were examined by scanning-electron microscopy and transmission-electron microscopy of secondary-carbon replicas.

3. RESULTS

3.1 Crack-Growth Data

In dry air and vacuum, frequency and wave-form had little effect on rates of crack growth under cyclic stress at constant ΔK ; differences between rates of crack growth in air and vacuum were small. Plotting da/dN versus ΔK on log scales, the air and vacuum data fell within a narrow scatter band which approximated to a linear relationship over the range of stress intensity between ~20 and ~60 MPa m^{1/2} (Fig. 1a-d); tests in hydrogen were restricted to this range of ΔK . The hydrogen environment produced large crack-growth rates, compared with the 'inert' environments, which were very sensitive to wave-form and frequency (Fig. 1a-d—each point is the average of at least three tests.) For given stress intensities and wave-forms, a decrease of two orders of magnitude in frequency produced an increase of roughly one order of magnitude in rate of crack growth, with increases being a little larger at higher ΔK . For given stress intensities and frequencies, rates of crack growth increased with waveform in the order going from \square to \triangle to \square to \square . The influence of frequency and wave-form (except for \square) could be rationalised approximately on the basis that rates of crack growth in hydrogen (for a given ΔK) were proportional to the rise-time (i.e. crack-opening time) (Fig. 2); crack-closing time had some effect since, for the same rise-time, \square wave forms (slow unloading rates) generally produced significantly faster crack growth than \triangle or \triangle wave-forms. The predominant effect of rise-time on rates of crack growth has been reported for other materials and environments.^(3,4) Rates of crack growth under sustained load in hydrogen and mercury environments are shown as functions of stress intensity in Figure 3; crack growth in mercury was two to three orders of magnitude faster than in (13.3 kPa) hydrogen. For \square wave-forms, where crack growth occurs under both sustained and rising loads, rates of crack growth per cycle were proportional to the time at maximum load (Fig. 4).

3.2 Fractography

3.2.1 Sustained-load Cracking in Hydrogen

Gradual changes in the appearance of the fracture-surfaces with gradually changing stress intensity were observed. At 'low' stress intensities (20–30 MPa m^{1/2}), crack growth was intercrystalline (i.e. along prior-austenite grain boundaries) and fairly smooth intercrystalline facets were observed. At 'intermediate' stress intensities (40–50 MPa m^{1/2}), many intercrystalline facets exhibited tear ridges and dimples (Fig. 5a,b). At 'high' stress intensities (65–75 MPa m^{1/2}), fractures were predominantly transcrystalline with dimpled surfaces (Fig. 6a,b). (Overload fracture—above K_{Ic} ~ 78 MPa m^{1/2}—was also dimpled and transcrystalline (Fig. 6c)). Similar observations have been reported for other steels cracked in gaseous hydrogen.⁽⁵⁾

3.2.2 Sustained-load Cracking in Liquid Mercury

Intercrystalline facets, virtually indistinguishable from those produced in hydrogen at 'intermediate' stress intensity, were observed (Fig. 7a,b), but there was little change in fracture-surface appearance† with stress intensity. For specimens additionally tempered to a lower

† The solubility of iron in mercury is negligible and, hence, fracture-surface topography is probably not affected by the presence of mercury on fracture surfaces.

strength (~ 1250 MPa) than 'usual' (all other tests used specimens with a proof stress of ~ 1460 MPa), sub-critical crack growth in liquid mercury produced a mixed transcrystalline/intercrystalline fracture with both areas almost entirely dimpled (Fig. 8a,b). For specimens tempered to a proof stress of ~ 1000 MPa, sub-critical crack growth in liquid mercury did not occur.

3.2.3 Fatigue in Dry Air

Crack growth was transcrystalline for all stress-intensities. At 'intermediate' ΔK ($30\text{--}50$ MPa $m^{1/2}$), quite well-defined fatigue striations were observed in some areas (Fig. 9); numerous steps, ridges, and small dimples were also observed and, hence, striations in many areas were short, irregular, and not well-defined. At low ΔK ($20\text{--}30$ MPa $m^{1/2}$), fracture surfaces were similar to those just described but striations were more difficult to resolve; at high ΔK (>60 MPa $m^{1/2}$), dimples predominated.

3.2.4 Fatigue in Hydrogen

Fracture-surface appearance depended on frequency and wave-form as well as on ΔK . At low ΔK and slow rates of loading, flat intercrystalline facets similar to those produced under sustained loading were observed. As rates of loading and ΔK increased, intercrystalline facets showed more evidence of local ductility (tear ridges, dimples) and the extent of transcrystalline cracking increased. Striations, although not well-defined, were evident in transcrystalline areas and on some intercrystalline facets. (Fig. 10).

4. DISCUSSION

4.1 Previous Explanations for Hydrogen Embrittlement (HE)

There is fairly general agreement⁽¹⁾ that the mechanism of HE of steels is the same regardless of the source of hydrogen. However, none of the previously proposed mechanisms of HE is generally accepted since none accounts for all the observations.⁽⁶⁾

One of the earliest theories for HE was based on precipitation of hydrogen at internal defects (e.g. voids, 'weak' particle/matrix interfaces); it has been proposed^(7,8) that the pressure developed by this precipitation is added to the applied stress and thus lowers the apparent fracture stress. This phenomenon probably contributes to embrittlement in 'charged' specimens but, by itself, does not account for many aspects of embrittlement.

Most mechanisms of HE have been based on supposed effects of dissolved hydrogen on the iron lattice. The most often-cited explanation, proposed by Oriani⁽⁹⁾ (expanding on theories by Troiano⁽¹⁰⁾ and others), is that dissolved hydrogen accumulates in regions of very high elastic stress within a few atomic distances from crack tips and thereby reduces the cohesive strength of the lattice. This hypothesis is based mainly on observations that hydrogen-induced failures often show little evidence of plastic deformation and result in flat intercrystalline or cleavage fracture facets. (In inert environments, crack growth is commonly associated with considerable deformation and often involves nucleation and growth of microvoids ahead of crack tips—dimpled fracture surfaces are often observed—and it is generally accepted that fracture occurs by slip processes at crack tips). In some cases, however, the presence of hydrogen can reduce tensile ductility without a change in fracture mode—only a change in dimple size is observed.⁽¹¹⁾ Similarly, Beachem⁽⁵⁾ observed that sub-critical crack growth of steels in gaseous hydrogen produced entirely dimpled fracture surfaces in some circumstances. He concluded that hydrogen-induced crack growth occurred by slip processes rather than by 'decohesion' and suggested that flat cleavage/intercrystalline facets also resulted from fracture by microscopic plasticity processes that were not readily apparent. Beachem therefore proposed that hydrogen diffused into the lattice just ahead of crack tips and there aided whatever deformation processes the lattice would allow. There is evidence that dissolved hydrogen may influence slip but generalizations about its effect are difficult to make; hydrogen may induce both increases and decreases in flow stress in different circumstances.⁽⁶⁾ Overall, it might be expected that dissolved hydrogen would not influence slip sufficiently to promote crack growth, since (a) hydrogen is quite mobile and can probably be swept along by moving dislocations⁽¹²⁾, and (b) there is already a high concentration of immobile solutes (and precipitates) in steels.

Many workers⁽¹³⁻¹⁶⁾ have noted that embrittlement of materials by hydrogen is similar to

liquid-metal embrittlement (LME). It has been proposed⁽¹⁶⁾ that chemisorption of liquid-metal or hydrogen atoms lowers the tensile (cohesive) strength of atomic bonds at crack tips so that crack growth occurs by repeated adsorption and tensile separation of bonds. The case for a common mechanism for HE and LME, based on chemisorption, is supported by the present studies. However, a 'reduced-cohesion' mechanism is *not* consistent with all the experimental observations and a new theory which explains both LME and HE is proposed here. (§ 4.3)

4.2 Comparison of HE and LME

Similarities between HE and LME are:

- (a) The hydrogen/iron couple has many of the characteristics of most liquid-metal/solid-metal embrittlement couples, viz. low mutual solubilities, little tendency to form compounds, similar electronegativities and strong binding energies between adsorbate and solid.⁽¹⁶⁾
- (b) Intercrystalline fractures are characteristic of both HE and LME, and fracture surfaces are indistinguishable in some cases (Figs 5, 7); dimpled transcrystalline fractures are sometimes observed after both HE and LME (Figs 6a, b; 8a, b).
- (c) The severity of both types of embrittlement generally increases with increasing strength. Steels with strengths above $\sim 1,200$ MPa are particularly susceptible to HE; for D6aC steel, sub-critical crack growth in mercury was not observed below about this strength in the present work.
- (d) The segregation of 'temper-embrittlement' elements (e.g. S, P, Sb, As, Sn) to prior-austenite grain boundaries enhances intercrystalline embrittlement by hydrogen and liquid metals.^(17, 18)
- (e) The addition of elements which form stable compounds with the solid to an embrittling liquid metal inhibits LME, e.g. the addition of a small amount of barium to mercury reduces the embrittlement of zinc by mercury.⁽¹⁹⁾ Similarly, traces of oxygen in the hydrogen inhibits HE.⁽²⁰⁾
- (f) The temperature-sensitivities of HE and LME are similar—maximum embrittlement generally occurs at a particular temperature, with reduced embrittlement at higher and lower temperatures.^(14, 16, 21)
- (g) Changes in the slip characteristics of the material from wavy glide to coplanar glide increases the severity of both HE and LME.^(22, 23)
- (h) Rates of crack growth about the same as those observed for D6aC steel in mercury have been reported⁽²⁴⁾ for a similar steel in partially dissociated hydrogen.

Known differences between HE and LME, e.g. much faster rates of crack growth in mercury compared to molecular hydrogen, increasing susceptibility to HE (but not LME) with decreasing strain rates, could arise because transport and adsorption kinetics are different. Other phenomena peculiar to HE, e.g. sub-surface initiation and growth of cracks, rates of crack growth controlled by diffusion of hydrogen through the lattice in some circumstances, do not necessarily indicate a different mechanism from LME since hydrogen could diffuse to, and chemisorb at, tips of internal cracks. Thus, it is concluded that HE and LME probably occur by the same basic process.

4.3 A new explanation for HE and LME

Crack growth occurs by either (a) tensile separation (decohesion) of atoms or (b) shear movement of atoms at crack tips, i.e. nucleation (and subsequent movement) of dislocations from crack tips, or emergence of dislocations at crack tips. For many materials, in inert environments, crack growth occurs by slip and the plastic strain is sufficient to produce some blunting at crack tips and to cause initiation and growth of voids ahead of cracks. Thus, crack growth involves coalescence of microvoids with crack tips and, as a result, dimpled fracture surfaces are observed. The present observations show that sub-critical crack growth of steel in liquid mercury and in hydrogen produces entirely dimpled fracture surfaces in some circumstances (Figs 6, 8), although dimples are generally smaller and shallower than those observed after fracture in air. Metallographic and fractographic observations of LME in other materials (e.g. aluminium single crystals)⁽²⁵⁾ show that considerable slip occurs around crack tips during crack growth in embrittling liquid-metal environments (much more deformation occurs in air) and that entirely dimpled fracture surfaces are produced. Thus, in many cases, crack growth

in embrittling environments almost certainly occurs by plastic flow rather than by decohesion of atoms at crack tips*. Furthermore, since transitions from dimpled to 'flat' fracture surfaces occur gradually (dimples become shallower and smaller and the proportion of fracture surface covered by dimples gradually decreases) with decreasing stress intensity or increasing strength, it is more probable that 'flat' fracture surfaces (Figs 5, 7) also result from crack growth by slip processes rather than by 'decohesion'. 'Flat' fracture surfaces would be observed (a) if dimples were too small/shallow to be resolved (the formation of dimples below the limit of resolution of replica techniques is quite probable), or (b) if fracture occurred by alternate shear at crack tips with insufficient strain ahead of cracks to nucleate voids. Beachem⁽⁵⁾ has also proposed that hydrogen-assisted crack growth occurs by plastic flow, as already mentioned.

LME is almost certainly caused by an effect of chemisorption at crack tips; mutual solubilities of LME couples are often negligible and rates of crack growth are so rapid (e.g. steel-mercury) that other processes would not have time to occur. The many similarities between LME and HE (4.2) suggest a common mechanism and it is proposed that sub-critical crack growth in liquid-metal/hydrogen environments, by plastic flow, can be explained on the basis that chemisorption of liquid-metal/hydrogen atoms facilitates nucleation of dislocations at crack tips. Atoms at surfaces (crack tips), in vacuum, have fewer neighbours than atoms in the interior and, hence, the lattice spacings in the first few atomic layers differ from those in the interior⁽²⁸⁾; such 'surface-lattice distortion' should hinder the nucleation (and egress) of dislocations at surfaces⁽²⁹⁾. Since chemisorption of environmental species effectively increases the number of neighbours around surface atoms, 'surface-lattice distortion' should be reduced⁽³⁰⁾ and nucleation of dislocations at surfaces (crack tips), should be facilitated by adsorption. Observations⁽³¹⁾ of iron-alloy surfaces in the presence of hydrogen, using field-ion microscopy, do indeed suggest that nucleation of dislocations is activated by adsorption of hydrogen.

4.4 Explanation of some aspects of HE

4.4.1 Environmental factors—effect of oxygen, solute elements on HE

The present considerations suggest that susceptibility to HE/LME (for a given stress intensity and microstructure) should be greater for larger chemisorption-induced reductions in 'surface-lattice distortion'; increased coverage by adsorbed species should also favour embrittlement since longer (surface) dislocation sources, which probably require lower activation stresses, may then be nucleated. Thus, the life of adsorbates on surfaces before reactions (such as compound formation, dissolution, diffusion into the solid) occur should influence the surface coverage at a particular instant and, hence, the nucleation of dislocations. An effect of surface coverage could account for the influence of hydrogen pressure, strain rate, temperature, and the presence of oxygen on HE. For example, the inhibition of HE by traces of oxygen in hydrogen environments probably occurs because oxygen adsorbs preferentially and rapidly produces an oxide at crack tips; oxygen itself does not facilitate crack growth, probably because its life in the adsorbed state is not long enough to produce a significant surface coverage by adsorbed oxygen at a particular instant. Chemisorption of species other than liquid-metal/hydrogen atoms could possibly facilitate generation of dislocations and some cases of stress-corrosion cracking could be explained on this basis.

The propensity for intercrystalline cracking in hydrogen/liquid-metal environments could be explained by preferential chemisorption of environmental species at grain boundaries. The presence of a high concentration of solute elements at prior-austenite boundaries could also be significant since the presence of such elements (S, As, P, Sb, Sn) can, by themselves, produce intercrystalline (temper-) embrittlement. Tin and antimony produce embrittlement (of steels) when in their liquid-metal state, and it is possible that temper-embrittlement, LME, and HE could all be manifestations of the same phenomenon (i.e. adsorption-activated dislocation

* It has been suggested⁽⁹⁾ that small areas of local plasticity could arise during fracture by 'decohesion', by plastic tearing of ligaments, unaffected by the environment, between advancing lobes of main cracks. However, it is very unlikely that crack growth occurs by a mixture of plastic flow and 'decohesion' to produce entirely dimpled fracture surfaces. Several workers^(26,27) have commented that, for fracture in general, crack growth by tensile separation of atoms at crack tips is probably uncommon.

nucleation) with differences arising because the source, mobility and 'potency' of embrittling species differ. A common mechanism would explain the 'co-operative' interaction between temper-embrittlement and HE/LME.

4.4.2 Ductile versus brittle behaviour

Previous considerations of ductile and brittle behaviour⁽³²⁾ have usually been based on a ' σ/τ ratio' criterion, where σ is the tensile stress required to rupture interatomic bonds at crack tips and τ is the shear stress required to move dislocations on slip planes intersecting crack tips. This criterion, however, only differentiates the relative tendencies for fracture by tensile separation of atoms and fracture by shear movement of atoms. Hence, it is considered inapplicable to those cases where both ductile and 'brittle' fracture occur by slip. Here, the distribution of slip around crack tips during crack growth should determine fracture behaviour. Extensive blunting at tips of cracks, in specimens below general yield, requires a general strain in the plastic zone around cracks and, hence, generally necessitates slip on at least five independent systems which freely interpenetrate and cross-slip⁽³³⁾; crack growth by (alternate) shear requires slip on only two slip planes intersecting crack tips.⁽³⁴⁾ The balance between crack growth and crack-tip blunting (both relax elastic strain energy around cracks) should therefore be determined by the relative proportions of slip on planes intersecting crack tips compared to 'general' slip ahead of cracks. Adsorption-activated nucleation (and subsequent movement) of dislocations from crack tips promotes the former and, hence, favours crack growth rather than crack-tip blunting*. Thus, increments of fatigue-crack growth, for given crack-opening displacements, are larger in hydrogen environments than in inert environments and both cyclic and sustained-load fractures in hydrogen have a 'less-ductile' appearance than fractures in inert environments. For sustained-load fracture, the amount of 'general' slip decreases with (a) more effective adsorption-induced generation of dislocations, (b) decreasing stress-intensity, and (c) increasing strength. The extent of void nucleation and growth ahead of cracks also decreases and, hence, fracture-surface dimples are either smaller/shallower or not observed (Figs 5-8). Where dimples are observed, they are often elongated, in the direction of crack growth, (Fig. 8a) probably due to the preferential advance of 'external' cracks (growth promoted by adsorption) towards internal voids (growing in vacuum—unless hydrogen diffuses or is swept by dislocations into voids). On fatigue-fracture surfaces, well-defined striations are observed after crack growth in air but *not* after cracking in hydrogen (Figs 9, 10). In many materials, 'brittle' striations are often observed after fatigue in 'aggressive' environments (e.g. hydrogen-charged iron⁽³⁵⁾, liquid-metal environments/aluminium⁽³⁶⁾, aqueous media/aluminium alloys) while 'ductile' striations are generally observed after fatigue in inert environments. Striations are often found on fatigue-fracture surfaces probably because, during unloading, slip behind the crack tip deforms part of the fracture surface produced during loading. Since crack-growth increments and crack-tip profiles are influenced by the environment, striation profiles are also affected (as illustrated in Fig. 11). Distributions and densities of dislocations adjacent to fracture surfaces should also be different after fatigue in inert and aggressive environments; observations consistent with the proposed model have been reported⁽³⁷⁾ for a nickel alloy fatigued in hydrogen and vacuum.

4.4.3 Effect of hydrogen on rates of crack growth

For fatigue in inert† environments, it is well-established that crack growth occurs only during loading as a result of slip at crack tips. Analyses of plastic-blunting/alternate-shear processes^(34, 38) show that crack-growth increments per cycle, da/dN , should be proportional to crack-tip-opening displacements, ΔCOD . Thus, $da/dN = B \cdot \Delta COD$; $COD \propto K^2/\sigma_y E$, and, hence, $da/dN \propto K^2$ relationships are often approximately observed (Fig. 1). The constant B can be considered as a measure of the balance between crack growth and crack-tip blunting during

* The effects of chemisorption on the lattice are 'screened out' within a few atomic distances of the surface and, hence, chemisorption does not influence the stress required for 'general' slip or usually affect properties other than fracture.

† Although there were probably very slight environmental effects in 'dry' air and 'vacuum', these environments were considered to be inert relative to hydrogen.

tensile loading. Thus B , and hence da/dN , depends on the environment (chemisorption), stress intensity, microstructure, etc. The influence of rise-time and stress intensity on rates of crack growth in hydrogen (Figs. 1, 2) can be explained on the basis that the effectiveness of hydrogen in promoting crack growth depends on the surface (crack-tip) coverage by adsorbed atoms during crack growth (4.4.1). Hydrogen transport/adsorption is less able to keep up with crack growth, and surface coverage is less, for higher rates of crack growth, da/dt ; in other words, B is smaller for faster loading rates and higher stress intensities.

The correlation between rates of crack growth and rise-time (Fig. 2) breaks down to some extent in that, for the same-rise time, \square wave-forms generally result in faster crack growth than \triangle and ∇ wave-forms. This effect probably occurs because the rates of unloading have a slight influence on crack growth. Since initial unloading displacements are elastic, there is probably a pause after peak load before reverse plastic deformation occurs around crack tips; crack growth during a pause of the order of 2% of the unloading period (estimated from square-wave data) would account for the results.

Other factors to be considered are the influence of environment on (a) the 'effective' COD , i.e. the range of COD over which plastic flow occurs—this should be greater in hydrogen than in air/vacuum, and (b) the amount of crack closure—dislocation egress behind crack tips during unloading could be affected by the environment and this, in turn, could influence crack growth.

4.4.4 Relationships between Sustained- and Cyclic-Load Cracking

It has been suggested^(39, 40) that rates of 'corrosion-fatigue' can be obtained by adding a component due to fatigue in an inert environment to an environmental component computed from the sustained-load-cracking data and the cyclic-load profile. For \triangle , ∇ , and \square wave-forms, crack-growth rates predicted by this 'superposition' analysis were quite different from the measured rates, e.g. predicted rates were about five times too slow at low ΔK . Various modifications to the 'superposition' analysis did not reveal any simple correlation between rates of sustained- and cyclic-load cracking, suggesting that there was a synergistic interaction (more marked at lower ΔK) between environment and rising load. (Similar results have been reported for other environment-material systems.) Quantitative correlations would not be expected on considering that increments of crack growth during fatigue and 'corrosion-fatigue' are controlled by increments of crack-opening displacement, while sustained-load cracking occurs under a constant COD . However, since cracking in hydrogen under both cyclic and sustained load probably involves adsorption-activated slip, qualitative relations between these processes should usually be observed, e.g. environmental factors which produce faster sustained-load cracking should also increase rates of 'corrosion-fatigue'.

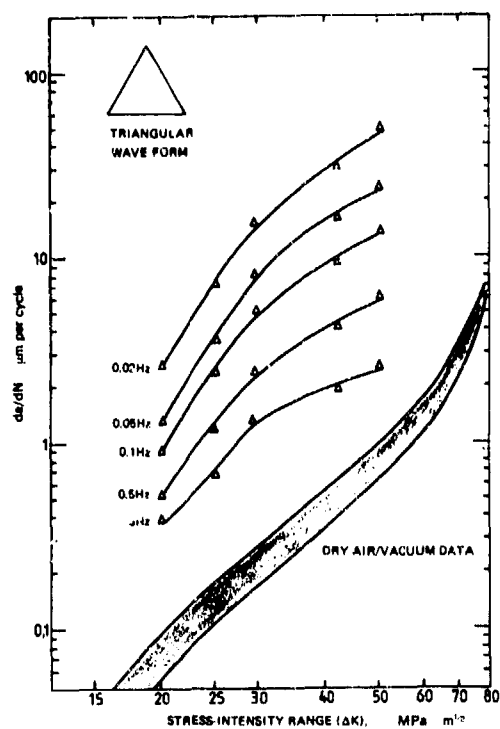
For square-wave loading, rates of fatigue-crack growth in hydrogen could be predicted to some extent by adding a 'corrosion-fatigue' component (i.e. crack growth during rising load in hydrogen) to a sustained-load cracking component (crack growth during the hold time at K_{max}). (Crack growth does not occur at K_{min} which is less than $K_{I,cc}$.) Predicted rates were in reasonable agreement with measured rates at low ΔK but were two to three times too high at high ΔK . The discrepancy at high ΔK probably occurs because the effective hydrogen pressure at the crack tip after a rapid increment of crack growth during rising load is lower than the nominal hydrogen pressure. Residual stresses around crack tips during sustained and cyclic-load crack will also be different and could influence rates of crack growth.

5. CONCLUSIONS

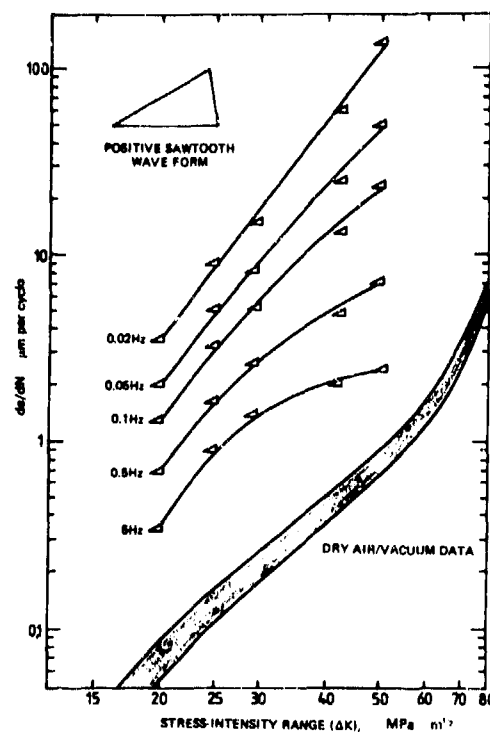
1. Comparison of hydrogen embrittlement and liquid-metal embrittlement suggests a common mechanism of crack growth.
2. Observations indicate that crack growth in embrittling environments generally occurs by plastic flow rather than by 'decohesion' of atoms.
3. Hydrogen embrittlement and liquid-metal embrittlement can be explained on the basis that chemisorption of hydrogen/liquid-metal atoms facilitates nucleation of dislocations at crack tips.
4. Rates of fatigue-crack growth in hydrogen are proportional to rise-times (rates unloading have only small effects); quantitative correlations between rates of cyclic- and sustained-load cracking were not observed.

REFERENCES

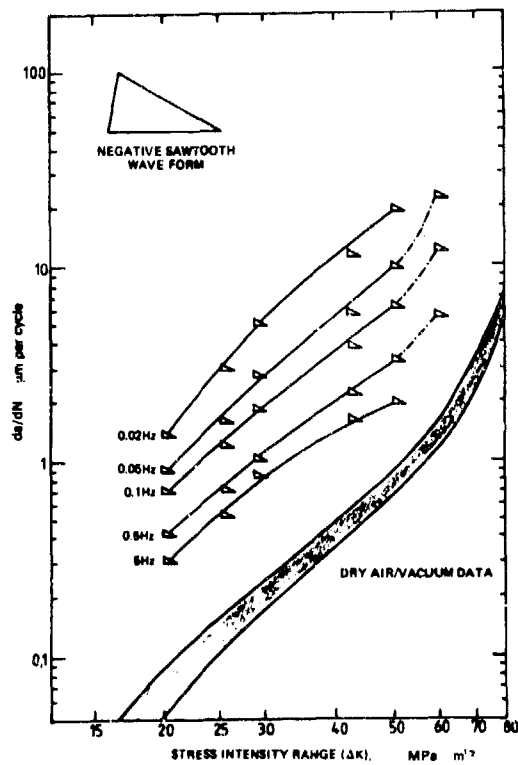
1. 'Effect of Hydrogen on Behaviour of Materials', ed. A. W. Thompson and I. M. Bernstein, Publ. Met. Soc. AIME, 1975.
2. 'Hydrogen in Metals', ed. I. M. Bernstein and A. W. Thompson, Publ. ASM Metals Park, 1974.
3. R. J. Selines and R. M. Pelloux, *Met. Trans.*, 1972, **3**, 2525.
4. J. M. Barson, p. 424, 'Corrosion Fatigue: Chemistry, Mechanics, and Microstructure', Ed. O. F. Devereux, A. J. McEvily, and R. W. Staehle, Publ. NACE, 1972.
5. C. D. Beachem, *Met. Trans.*, 1972, **3**, 437.
6. M. R. Louthan, Jr. and R. P. McNitt, p. 496, ref. 1.
7. C. A. Zapffe and C. E. Sims, *Metals and Alloys*, 1940, **11**, 145 and 177.
8. M. R. Louthan, Jr., p. 53, ref. 2.
9. R. A. Oriani, *Ber. Bunsenges, Phys. Chem.*, 1972, **76**, 848.
10. A. R. Troiano, *Trans., ASM*, 1960, **52**, 54.
11. A. W. Thompson, p. 467, ref. 1.
12. J. K. Tien, p. 309, ref. 1.
13. W. H. Johnson, *Proc. Roy. Soc.*, 1875, **23**, 168.
14. D. P. Williams and H. G. Nelson, *Met. Trans.*, 1970, **1**, 63.
15. I. M. Bernstein, *Mat. Sci. and Eng.*, 1970, **6**, 1.
16. M. H. Kamdar, *Progress in Materials Science*, 1973, **15**, 289.
17. K. Yoshino and C. J. McMahon, Jr., *Met. Trans.*, 1974, **5**, 363.
18. S. Dinda and W. R. Warke, *Mat. Sci. and Eng.*, 1976, **24**, 199.
19. A. R. C. Westwood, p. 407, 'Strengthening Mechanisms—Metals and Ceramics', ed. J. J. Burke, N. L. Reed, and V. Weiss, Publ. Syracuse Univ. Press, 1966.
20. G. G. Hancock and H. H. Johnson, *Trans. AIME*, 1966, **236**, 513.
21. K. Farrell and A. G. Quarrell, *J.I.S.T.*, 1964, **198**, 1002.
22. N. S. Stoloff, R. G. Davies, and T. L. Johnston, p. 613, 'Environment-Sensitive Mechanical Behaviour', ed. A.R.C. Westwood and N. S. Stoloff, Publ. Gordon and Breach, 1966.
23. B. C. Odegard, J. A. Brooks and A. J. West, p. 116, ref. 1.
24. J. D. Frandsen and H. L. Marcus, p. 233, ref. 1.
25. S. P. Lynch, ARL Report No. 102, 1977 and 4th Int. Conf. on Fracture, Waterloo, 1977.
26. N. J. Petch, p. 351, 'Fracture: An Advanced Treatise, Vol. 1', ed. H. Liebowitz, Publ. Academic Press, 1968.
27. C. D. Beachem, '2nd Int. Conf. on Mechanical Behaviour of Materials', Boston, 1976.
28. R. M. Latanision, p. 185, ref. 4.
29. R. L. Fleischer, *Acta Met.* 1960, **8**, 598.
30. H. H. Uhlig, p. 312, 'Metal Interfaces', Publ. ASM, 1952.
31. J. A. Clum, *Scripta Met.*, 1975, **9**, 51.
32. A. Kelly, W. R. Tyson and A. H. Cottrell, *Phil. Mag.*, 1967, **15**, 567.
33. A. Kelly, §3.3 'Strong Solids', Publ. Clarendon Press, 1973.
34. R. M. N. Pelloux, *Eng. Frac. Mech.*, 1970, **1**, 697.
35. D. A. Ryder, 'The Elements of Fractography', Publ. AGARD-AG-155-71, 1971.
36. S. P. Lynch, in 'Fatigue Mechanisms', ASTM STP to be published.
37. J. D. Frandsen, N. E. Paton, and H. L. Marcus, *Met. Trans.*, 1974, **5**, 1655.
38. R. J. Donahue, H. McL. Clark, P. Atanmo, R. Kumble, and A. J. McEvily, *Int. J. Frac. Mech.*, 1972, **8**, 209.
39. R. P. Wei and J. D. Landes, *Mat. Res. and Sids.*, 1969, **9**, 25.
40. W. W. Gerberich, J. P. Birat, and V. F. Zackay, p. 396, ref. 4.



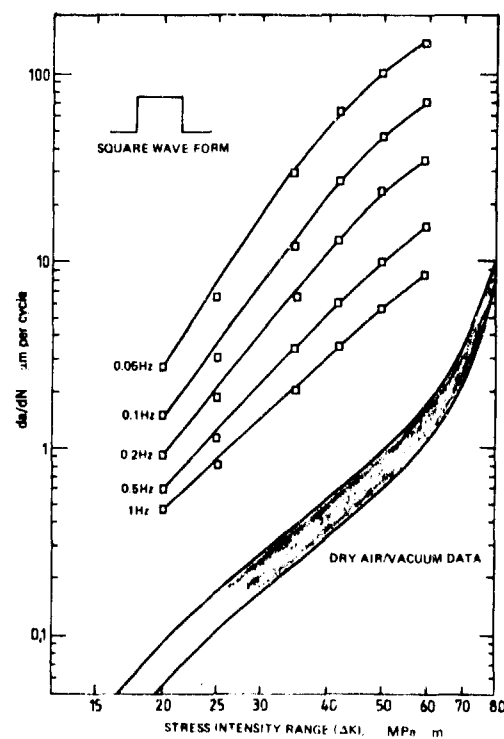
(a)



(b)



(c)



(d)

Fig. 1. Graphs of rate of fatigue-crack growth per cycle (da/dN) versus stress-intensity range (ΔK) showing effect of cyclic frequency for (a) triangular-wave forms, (b) positive-sawtooth-wave forms, (c) negative-sawtooth-wave forms, and (d) square-wave forms, in a hydrogen gas environment. Rates of crack growth in dry air and vacuum (shaded band) are relatively insensitive to frequency and wave form.

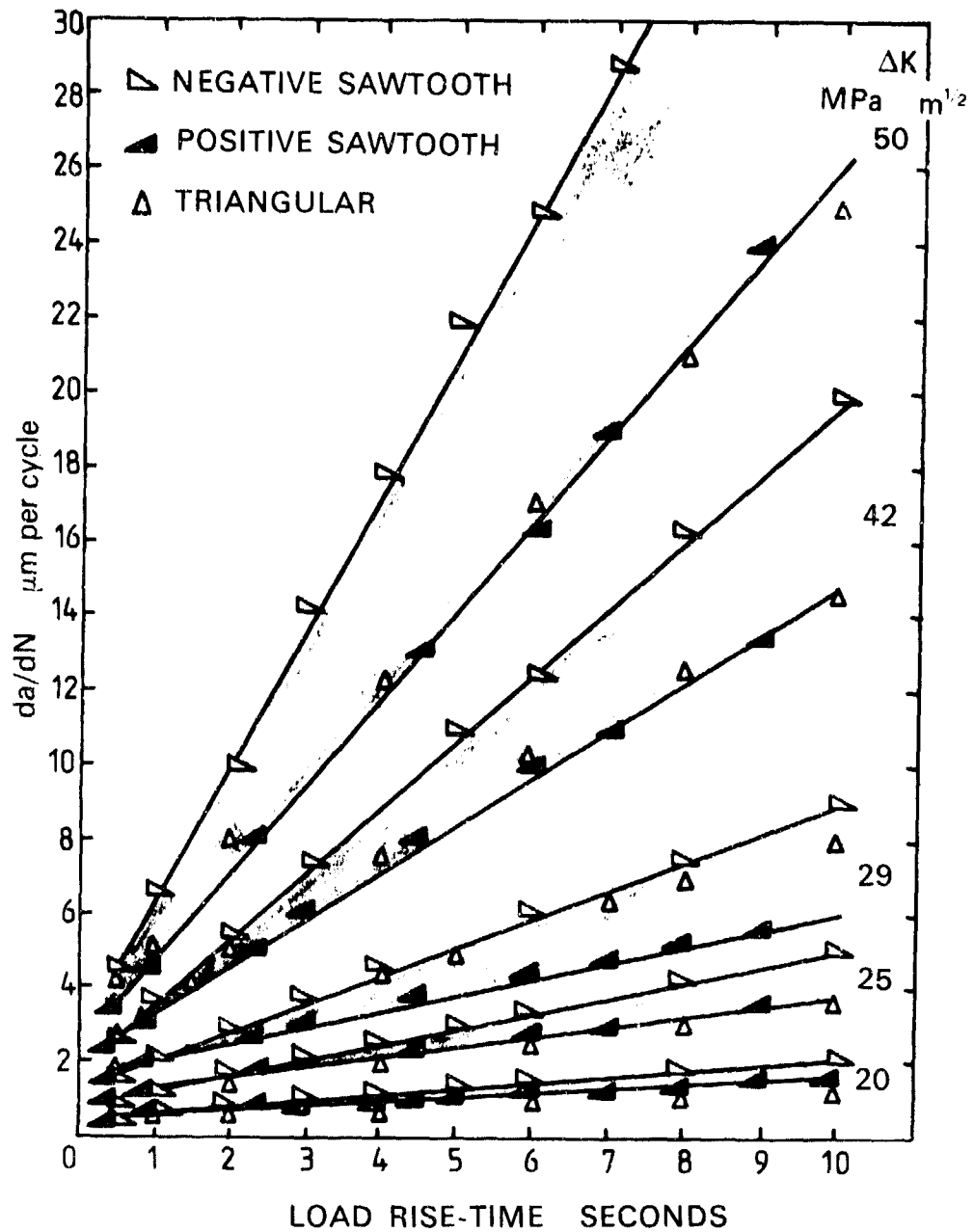


Fig. 2 Graph of rate of fatigue-crack growth per cycle (da/dN), in hydrogen gas, versus load-rise time showing that, for a given ΔK , da/dN is approximately proportional to the rise-time. Rates of unloading have a small effect in that, for the same rise times ∇ wave forms generally produce slightly faster crack growth than \blacktriangle or \triangle wave forms.

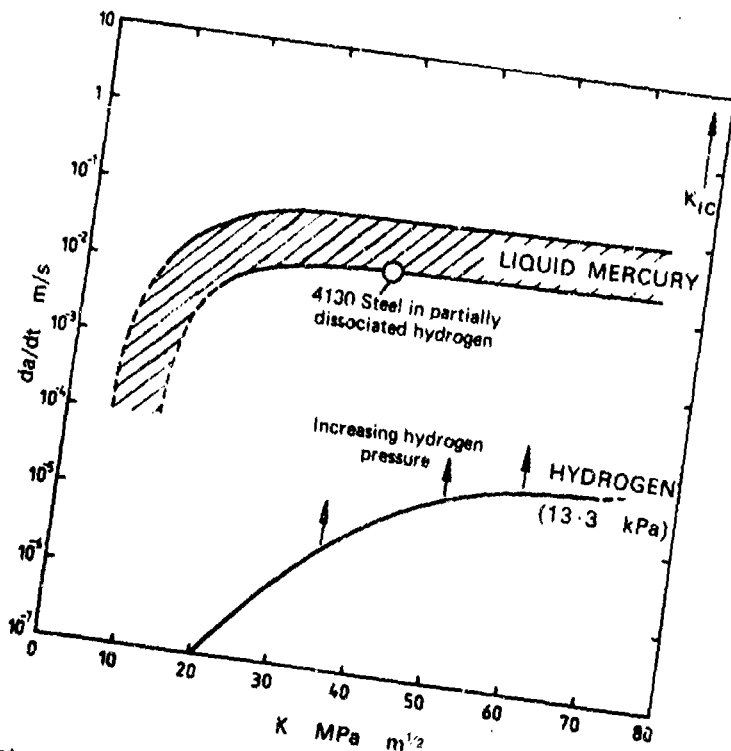


Fig. 3 Effect of stress intensity (K) on rates of sustained-load crack growth (da/dt) in low pressure (13.3 kPa) hydrogen and liquid mercury environments.

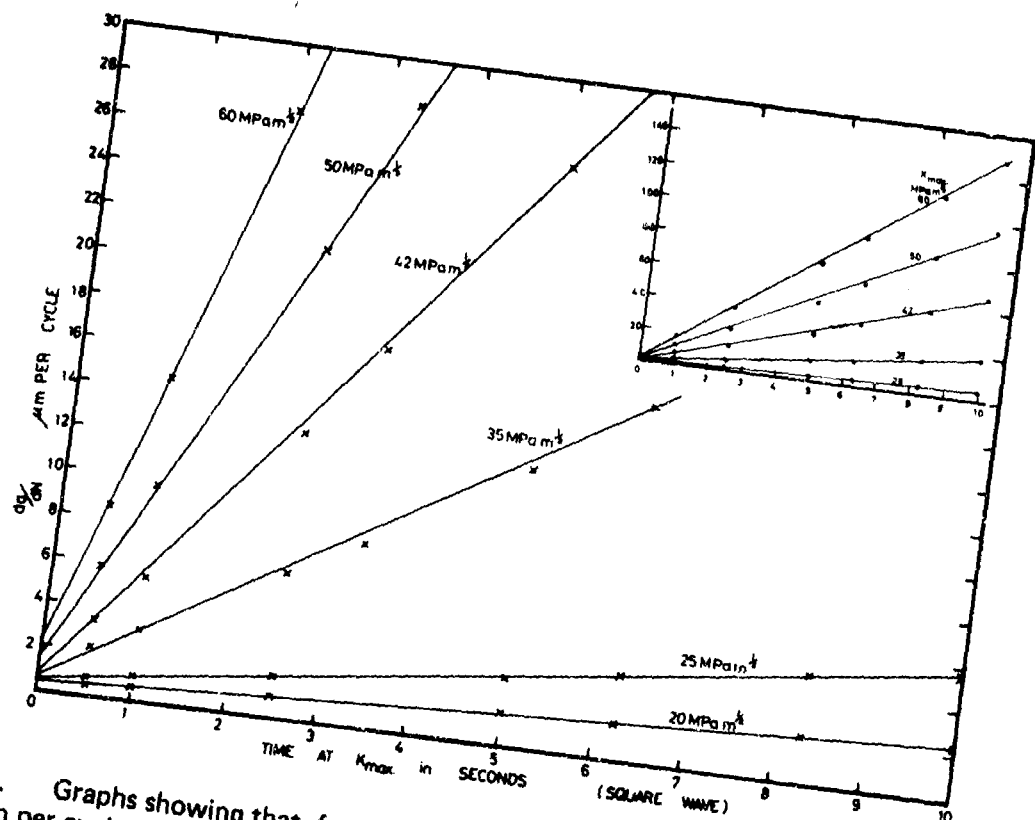
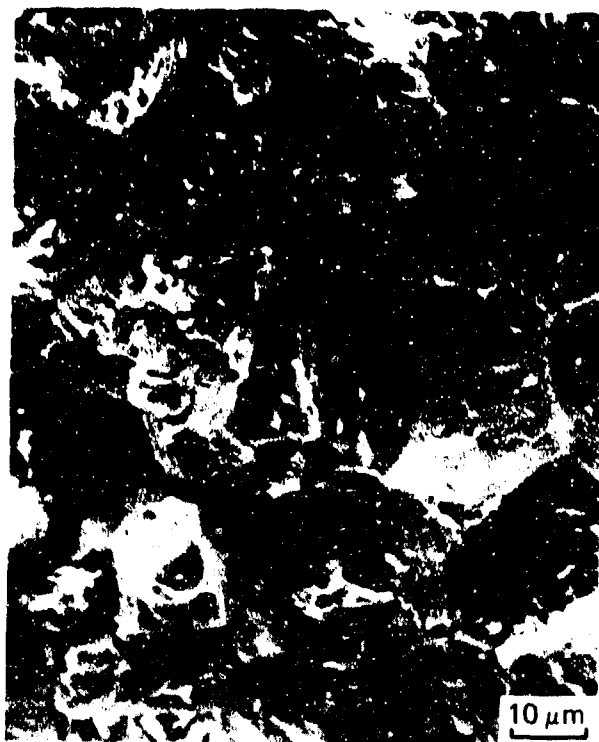


Fig. 4. Graphs showing that, for square-wave cycling in hydrogen, rates of fatigue-crack growth per cycle (da/dN) for a given ΔK are proportional to the time at K_{max}.



(a)

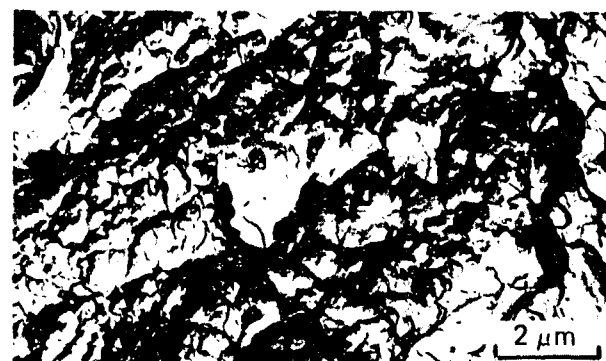


(b)

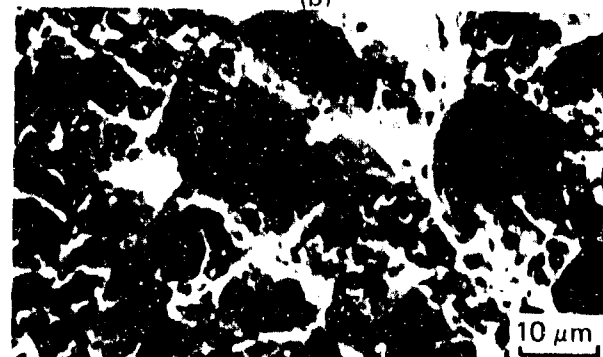
Fig. 5. Fractographs (a) – SEM, (b) – EM) after sustained-load cracking in hydrogen at 'intermediate' stress intensities ($40 - 50 \text{ MPa m}^{1/2}$) showing flat and dimpled intercrystalline facets.



(a)



(b)



(c)

Fig. 6. Fractographs (a) – SEM, (b) – EM after sustained-load cracking in hydrogen at high stress intensities ($65 - 75 \text{ MPa m}^{1/2}$) showing predominantly dimpled transcrystalline fracture; (c) – SEM shows dimpled transcrystalline fracture produced by overload in dry air ($K_{IC} - 78 \text{ MPa m}^{1/2}$).



(a)



(b)

Fig. 7. Fractographs ((a) – SEM, (b) – EM) after sub-critical crack growth in liquid mercury at 'intermediate' stress intensities showing intercrystalline facets indistinguishable from those produced by cracking in hydrogen (cf. Fig. 5 a, b).



(a)



(b)

Fig. 8. Fractographs (EM) after sub-critical crack growth in liquid mercury at intermediate stress intensities for a specimen tempered to a lower strength than 'normal' (see text) showing (a) area of dimpled transcrystalline fracture and (b) area of dimpled intercrystalline fracture.

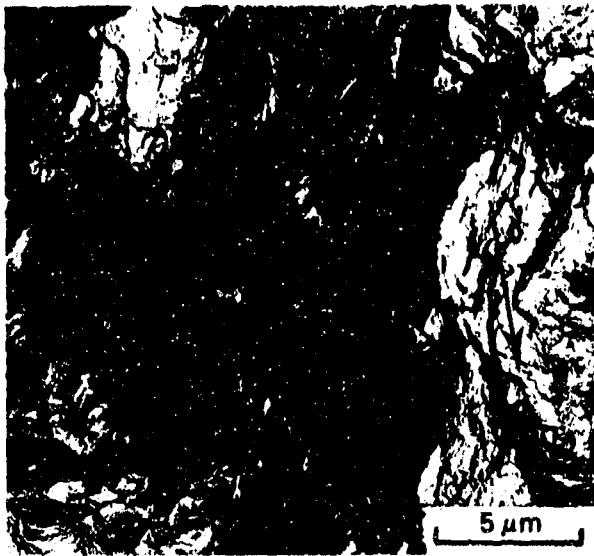


Fig. 9. Fractograph (EM) after fatigue-crack growth in dry air ($\Delta K = 35 \text{ MPa m}^{1/2}$) showing striations, small dimples and tear ridges.



Fig. 10. Fractograph (EM) after fatigue crack growth in hydrogen ($\Delta K = 25 \text{ MPa m}^{1/2}$, 1 Hz, Δ wave-form) showing intercrystalline and transcrystalline areas with signs of striations in both regions.

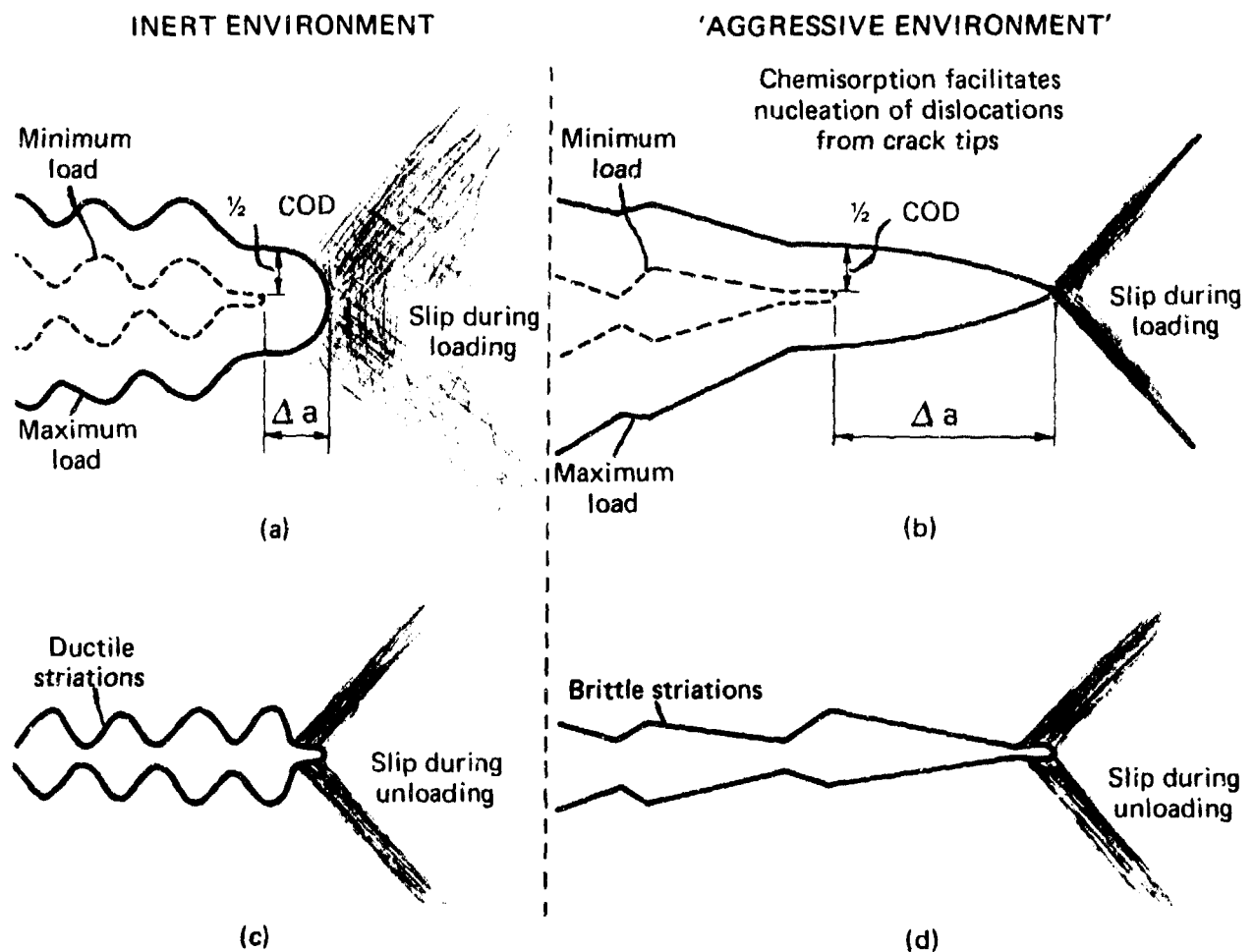


Fig. 11. a, b. Diagrams illustrating effect of environment on slip distribution around crack tips, crack-tip profiles, and crack-growth increments per cycle (Δa) for the same crack-tip-opening displacements (ΔCOD) during fatigue-crack-growth. During unloading, slip behind crack tips produces (c) 'ductile' striations, and (d) 'brittle' striations, on fracture surfaces.

DOCUMENT CONTROL DATA SHEET

Security classification of this page: Unclassified

- | | |
|--|--|
| <p>1. Document Numbers</p> <p>(a) AR Number:
AR-001-273</p> <p>(b) Document Series and Number:
Materials Report 103</p> <p>(c) Report Number:
ARL-Mat-Report-103</p> | <p>2. Security Classification</p> <p>(a) Complete document:
Unclassified</p> <p>(b) Title in isolation:
Unclassified</p> <p>(c) Summary in isolation:
Unclassified</p> |
|--|--|

3. Title: **MECHANISMS OF HYDROGEN EMBRITTLEMENT: CRACK GROWTH IN A LOW-ALLOY ULTRA-HIGH-STRENGTH STEEL UNDER CYCLIC AND SUSTAINED STRESSES IN GASEOUS HYDROGEN**

- | | |
|--|--|
| <p>4. Personal Author(s):
S. P. Lynch
N. E. Ryan</p> | <p>5. Document Date:
May, 1978</p> |
| <p>6. Type of Report and Period Covered:</p> | |

- | | |
|---|---|
| <p>7. Corporate Author(s):
Aeronautical Research Laboratories</p> | <p>8. Reference Numbers</p> <p>(a) Task: Air 72/8</p> <p>(b) Sponsoring Agency:</p> |
|---|---|

9. Cost Code:
35 1610

- | | |
|---|---|
| <p>10. Imprint:
Aeronautical Research Laboratories,
Melbourne</p> | <p>11. Computer Program(s)
(Title(s) and language(s)):
Not Applicable</p> |
|---|---|

12. Release Limitations (of the document):
Approved for Public Release

12-0. Overseas:	No.	P.R.	I	A	B	C	D	E
-----------------	-----	------	---	---	---	---	---	---

13. Announcement Limitations (of the information on this page):
No Limitation

- | | |
|---|---|
| <p>14. Descriptors:</p> <p>Hydrogen Embrittlement High Strength Steels</p> <p>Crack Propagation Fractography</p> <p>Fatigue (Materials) Fracturing</p> <p>Stress Corrosion</p> | <p>15. Cosati Codes:</p> <p>2012,</p> <p>1113</p> |
|---|---|

16. **ABSTRACT**

Rates of crack growth in a low-alloy ultra-high-strength steel (D6aC) under cyclic and sustained stresses have been measured as functions of stress-intensity, for different cyclic wave-forms and frequencies, in low pressure (13.3 kPa) hydrogen, dry air, and vacuum (10⁻³ Pa) environments; sustained-load cracking in liquid mercury was also studied.

Frequency and wave-form had large effects on rates of fatigue-crack growth in hydrogen but little influence on fatigue in air and vacuum. For triangular wave-forms, rates of crack growth in hydrogen were determined mainly by the stress-intensity range and the load-rise time. For square-wave loading, rates of crack growth in hydrogen were proportional to the time at maximum load. Quantitative relationships between rates of cracking under sustained and cyclic loads were not found.

Many similarities between hydrogen-embrittlement and liquid-metal embrittlement (e.g. surfaces of the intercrystalline fractures induced by hydrogen and mercury were sometimes indistinguishable) suggested that the mechanism of embrittlement is basically the same in both cases. It is considered that previous explanations for embrittlement are not consistent with the present fractographic observations (e.g. dimpled transcrystalline fractures were sometimes observed after crack growth in mercury and hydrogen). The present results suggest that the effects of hydrogen and liquid-metal environments on crack growth can generally be explained on the basis that chemisorption influences interatomic bonds/spacings at surfaces (crack tips) and thereby facilitates nucleation of dislocations at crack tips. Some aspects of hydrogen embrittlement are discussed in terms of the proposed model.

DISTRIBUTION

AUSTRALIA

DEPARTMENT OF DEFENCE

	Copy No.
Central Office	
Chief Defence Scientist	1
Executive Controller, ADSS	2
Superintendent, Defence Science Administration	3
Defence Library	4
JIO	5
Assistant Secretary, DISB	6-21
Australian Defence Scientific and Technical Representative (UK)	22
Counsellor, Defence Science (USA)	23
Aeronautical Research Laboratories	
Chief Superintendent	24
Superintendent, Materials Division	25
Materials Divisional File	26
Authors: S. P. Lynch	27
N. E. Ryan	28
Librarian	29
Materials Research Laboratories	
Librarian	30
Defence Research Centre	
Librarian	31
Central Studies Establishment Information Centre	
Librarian	32
Engineering Development Establishment	
Librarian	33
RAN Research Laboratory	
Librarian	34
Navy Office	
Naval Scientific Adviser	35
Army Office	
Army Scientific Adviser	36
Royal Military College (Librarian)	37
US Army Standardisation Group	38
Air Force Office	
Air Force Scientific Adviser	39
Aircraft Research and Development Unit	40
Engineering (CAFTS) Librarian	41
D. Air Eng.	42
HQ Support Command (SENGSO)	43

DEPARTMENT OF PRODUCTIVITY

Government Aircraft Factories

Library 44

DEPARTMENT OF TRANSPORT

Director-General/Library 45

Airworthiness Group (Mr R. Ferrari) 46

STATUTORY, STATE AUTHORITIES AND INDUSTRY

Australian Atomic Energy Commission (Director) NSW 47

CSIRO Central Library 48

CSIRO Tribophysics Division (Director) 49

Qantas, Library 50

Trans Australia Airlines, Library 51

Gas and Fuel Corporation of Vic. (Research Director) 52

Ministry of Fuel and Power (Secretary) Victoria 53

SEC Herman Research Laboratory (Librarian) Vic. 54

SEC of Queensland, Library 55

Ansett Airlines of Australia, Library 56

Australian Paper Manufacturers (Dr Norman) 57

BHP Melbourne Research Laboratories, Library 58

BP Australia Ltd (Librarian) Vic. 59

Commonwealth Aircraft Corporation (Manager) 60

Commonwealth Aircraft Corporation (Manager of Engineering) 61

Hawker de Havilland Pty Ltd (Librarian) Bankstown 62

Hawker de Havilland Pty Ltd (Manager) Lidcombe 63

ICI Australia Ltd, Library 64

Institute of Fuel, Australian Branch (Secretary) 65

Petroleum Information Bureau (Australia) 66

Rolls Royce of Australia Pty Ltd (Mr Mosley) 67

Shell Chemical (Australia) Pty Ltd (Mr G. R. Bamford) 68

H. C. Sleigh Ltd, Technical Dept., Library 69

UNIVERSITIES AND COLLEGES

Adelaide Barr Smith Library 70

Professor R. Miller, Chem. Eng. & Mat. Sci. 71

Australian National Library 72

Flinders Library 73

James Cook Library 74

La Trobe Library 75

Melbourne Engineering Library 76

Dr C. J. Osborn Metallurgy 77

Monash Library 78

Professor I. J. Polmear 79

Newcastle Library 80

New England Library 81

New South Wales Physical Science Library 82

Professor L. H. Keys 83

Queensland Library 84

Professor G. Chadwick, Mining & Met. 85

Tasmania Engineering Library 86

Professor A. R. Oliver, Civil and Mech. Eng. 87

West. Australia Library 88

RMIT Library 89

Principal 90

Head, School of Metallurgy 91

CANADA		
CAARC Co-ordinator, Materials		92
Energy, Mines and Resources Dept., Physics and Metallurgy Research Laboratories (Dr A. Williams)		93
NRC, National Aeronautics Est. Library		94
UNIVERSITIES		
McGill	Library	95
Toronto	Institute of Aerodynamics	96
FRANCE		
AGARD	Library	97
ONERA	Library	98
Service de Documentation Technique de L'Aeronautique		99
GERMANY		
Dr W. Schütz, Industrieanlagen-Betriebsgesellschaft Ottobrunn, Mblt. 8012		100
INDIA		
CAARC Co-ordinator Materials		101
Indian Institute of Science, Library		102
Indian Institute of Technology, Library		103
National Aeronautical Laboratory (Director)		104
ISRAEL		
Technion- Israel Institute of Technology (Professor J. Singer)		105
ITALY		
Associazione Italiana di Aeronautica and Astronautica (Professor A. Evia)		106
JAPAN		
National Aerospace Laboratory, Library		107
UNIVERSITIES		
Tohoku (Sendai)	Library	108
Tokyo	Institute of Space and Aerospace	109
NETHERLANDS		
Central Organisation for Applied Science Research in the Netherlands TNO, Library		110
National Aerospace Laboratory (NLR) Library		111
NEW ZEALAND		
Air Dept. RNZAF, Aero. Documents Section		112
UNIVERSITIES		
Canterbury	Library	113
	Mr F. Fahy, Mechanical Engineering	114
Auckland	Professor A. Titchener	115
SWEDEN		
Aeronautical Research Institute		116
Chalmers Institute of Technology, Library		117
Kungl. Tekniska Hogskolans		118
SAAB, Library		119
Research Institute of the Swedish National Defence		120

SWITZERLAND

Brown Boverie (Management Chairman) 121

UNITED KINGDOM

Mr A. R. G. Brown ADR/MAT (MEA) 122
Ministry of Power (Chief Scientist) 123
CAARC NPL (Secretary) 124
Royal Aircraft Establishment Library, Farnborough 125
Royal Aircraft Establishment Library, Bedford 126
Royal Armament Research and Development Est. Library 127
Admiralty Materials Labs (Dr R. G. Watson) 128
National Engineering Labs (Superintendent) 129
National Gas Turbine Est (Director) 130
British Library, Science Reference Library 131
British Library, Lending Division 132
CAARC Co-ordinator Materials 133
Aircraft Research Association, Library 134
British Non-Ferrous Metals Association 135
C. A. Parsons Library, and Mr A. D. Batte 136
Central Electricity Generating Board 137
Electrical Power Storage Ltd (Director of Fuel Cell Research) 138
Energy Conversion Ltd (Research Director) 139
Institute of Fuel (Secretary) 140
Fulmer Research Institute Ltd (Research Director) 141
Science Museum Library 142
Welding Institute, Library 143

UNIVERSITIES AND COLLEGES

Bristol Dr W. J. Plumbridge, Met. Dept. 144
Birmingham Dr J. Beevers, Dept. Phys. Met. and Sci. of Mat. 145
Cambridge Dr J. Knott, Metallurgy Dept. 146
Professor R. Honeycombe, Metallurgy Dept. 147
Dr K. J. Miller, Engineering 148
Manchester Dr G. Lorimer, Metallurgy Dept. 149
Manchester Institute of Sci. and Tech. D. A. Ryder, Metallurgy Dept. 150
Nottingham Professor J. S. Leach, Metallurgy 151
Oxford Professor J. W. Christian, Metallurgy Dept. 152
Dr J. W. Martin, Metallurgy Dept. 153
Salford Dr P. E. Thompson 154
Southampton Library 155
Cranfield Ins. of Tech. Library 156
Imperial College, London Dr P. R. Swan, Materials Science 157
Leeds Professor J. Nutting, Houndsworth School of Applied Science 158
Dr J. C. Scully, Houndsworth School of Applied Science 159
Liverpool Professor J. Stringer, Materials Science 160
Newcastle-upon-Tyne Professor R. N. Parkins, Metallurgy 161
Sheffield Professor G. W. Greenwood, Metallurgy 162

UNITED STATES OF AMERICA

NASA Scientific and Technical Information Facility 163
Sandia Group (Research Organisation) 164
American Institute of Aeronautics and Astronautics 165
Applied Mechanics Reviews 166
The John Cerar Library 167

The Chemical Abstracts Service	168
Boeing Co. Head Office	169
Boeing Co. Industrial Production Division	170
General Electric (Aircraft Engine Group)	171
Lockheed Aircraft Co. (Director)	172
Metals Abstracts	173
McDonnell Douglas Corp. (Director)	174
United Technologies Corporation (Director)	175
United Technologies Corporation, Pratt and Whitney Group	176
Battelle Memorial Institute, Library	177
Ames Research Centre (Dr H. G. Nelson)	178
Westinghouse Research Labs (Dr S. J. Hudak)	179
US Steel Applied Research Labs (Dr J. M. Barsom)	180
US Naval Research Labs, Engineering Materials Division (Dr C. D. Beachem)	181

UNIVERSITIES AND COLLEGES

Brown	Professor J. R. Rice	189
Carnegie Mellon	Professor I. M. Bernstein	182
Connecticut	Professor A. J. McEvily	183
Minnesota	Professor W. W. Gerberich	184
Pennsylvania	Professor C. J. McMahon	185
Rensselaer	Professor N. S. Stoloff	186
Lehigh	Professor R. P. Wei	187
Illinois I. T.	Professor Warke	188

Spares

190-200